Induced magnetism in Cu nanoparticles embedded in Co

P. Swaminathan
Department of Materials Science and Engineering, University of Illinois at Urbana-Champaign, Urbana, Illinois 61801, USA

R. A. Rosenberg and G. K. Shenoy
Advanced Photon Source, Argonne National Laboratory, Argonne, Illinois 60439, USA

J. S. Palmer and J. H. Weaver[a)]
Department of Materials Science and Engineering, University of Illinois at Urbana-Champaign, Urbana, Illinois 61801, USA

(Received 20 September 2007; accepted 17 October 2007; published online 14 November 2007)

One-dimensionally confined nonferromagnetic layers of Cu grown between ferromagnetic layers of Co have an average induced magnetic moment that decreases with Cu film thickness. We studied the effects of changing the nature of confinement to three dimensions by embedding Cu nanoparticles in a Co matrix and measuring the induced moments using x-ray magnetic circular dichroism. The nanoparticle spin moments were more than twice that of films of comparable thickness due to the three dimensional confinement and greater interfacial area. © *2007 American Institute of Physics*. [DOI: 10.1063/1.2806236]

Nonmagnetic spacer layers grown between layers of magnetic materials exhibit an induced magnetic moment.[1–4] For example, Cu layers between Co possess an induced ferromagnetic moment.[1] Theoretical local spin density calculations show that the induced moment, mainly of the spin type, is maximum at the interface and drops to zero within 3–4 atomic layers from the interface.[5] Cu suppresses the magnetic moment of Co by hybridization of the 3*d* orbitals at the interface.[6] An oscillatory exchange coupling between the Co layers is seen, manifests as an oscillation in the magnetoresistance.[7] This finds application in spin based memory devices.[8] The average induced moment in Cu is inversely proportional to its thickness, an effect related to moments being mainly at the interface.

In this paper, we discuss induced magnetism in three dimensional Cu nanoparticles embedded in a matrix of Co. We show that the moment for nanoparticles of radii r is significantly higher than that in thin films of thickness $2r$ due to the greater interfacial area. This might lead to greater magnetoresistance in samples containing nanoparticles compared to thin films. The nanoparticles also suppress the spin moment in Co depending on the size and coverage. Using the elemental specificity of polarized x-ray absorption spectroscopy (XAS), we can compute the magnetic moment by studying the dichroism in the L edges of Cu and Co.[9] This technique, called x-ray magnetic circular dichroism (XMCD), refers to the difference in XAS obtained with the radiation polarized parallel and antiparallel to the magnetic moment. Orbital and spin magnetic moments can then be obtained from the difference spectra.[10,11] Since the contribution of the 3*d* electrons to the moment is greater than that of the 4*s* electrons, these moments correspond to those of the *d* electrons.[12]

To achieve three dimensional confinement, we condensed an inert Xe multilayer on Co and vapor deposited Cu onto it. Subsequent warm up formed nanoparticles which were delivered to the substrate after Xe removal. This process, called buffer-layer-assisted growth (BLAG), has been used to grow particles of a wide range of materials, usually with condensed rare gases as buffers.[13–16] Here, the samples were grown in an ultrahigh vacuum chamber with a base pressure below $\sim 1 \times 10^{-10}$ Torr. Samples for magnetic measurements were grown on GaAs wafers. A base layer of 100 Å Co was deposited onto the wafers at room temperature, forming a polycrystalline thin film. The Cu nanoparticles formed and delivered to the Co surface by BLAG were then capped with a 50 Å layer of Co at room temperature. The densities and sizes of the particles are controlled by the amount of Cu and thickness of Xe. Since particle formation is independent of the substrate,[13] clusters were grown simultaneously on *a*-C transmission electron microscopy (TEM) grids for structural characterization. We also grew Cu thin films at room temperature for comparison with the literature.[1] The Co base- and overlayer thicknesses were the same for the film samples.

TEM images were used to determine the average sizes and densities of the particles. Figure 1 shows representative images with their densities, average radii, and standard deviations listed. For a given amount of material, the particle density decreases with Xe thickness following a power law behavior.[14] Particles with the same average size and different

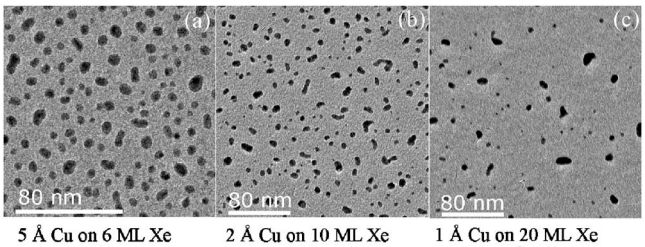

FIG. 1. TEM images of Cu nanoparticles that were grown on *a*-C TEM grids alongside samples prepared for XMCD measurements. The growth conditions, average particle sizes with standard deviations, and particle densities are given.

[a)]Electronic mail: jhweaver@uiuc.edu

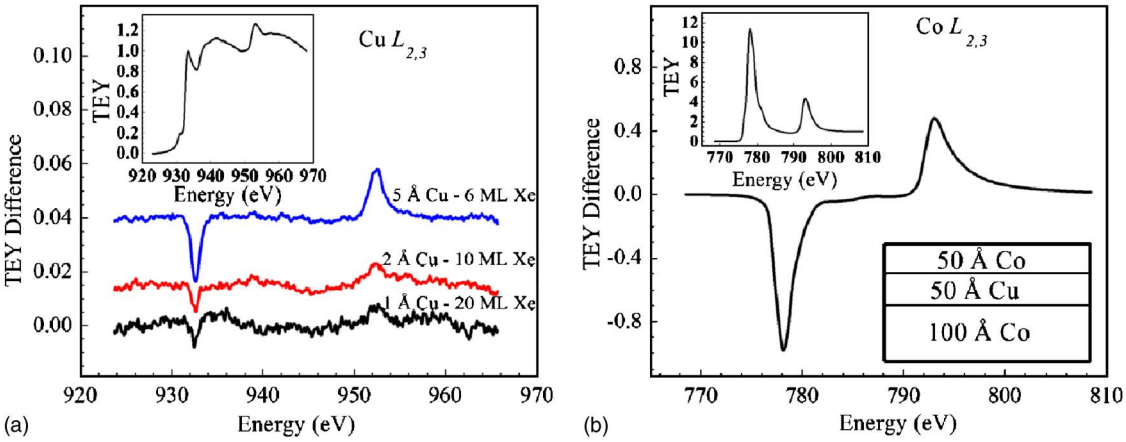

FIG. 2. (Color online) (a) L-edge XMCD spectra from the Cu nanoparticles, offset vertically for clarity. The inset shows a typical absorption spectrum. (b) L-edge spectrum from Co with its absorption spectrum in the inset for a Cu thin film sandwiched between Co. The areas under the L_3 and L_2 peaks were used to obtain the moments listed in Table I.

densities can be obtained by controlling the amount of material and Xe thickness, as shown in Figs. 1(b) and 1(c).

The XMCD measurements were carried out at sector 4 of the Advanced Photon Source using Beamline 4-ID-C. An undulator provided the left- and right-circular polarized x-rays with a polarization >96%. X rays were incident on the sample at a glancing angle of 15°, and all measurements were carried out at room temperature. The samples were magnetized by applying an ~200 Oe field. All data were obtained with the samples in the remanent state. Absorption measurements were carried out in the total electron yield mode. The polarization was switched at each photon energy in order to obtain intensities parallel and antiparallel to the sample magnetization. The difference in the spectra, XMCD, is magnetic in origin and proportional to the magnetization in the material.

Figure 2(a) shows L-edge XMCD spectra for the Cu nanoparticles with a typical absorption spectrum in the inset. Figure 2(b) shows the corresponding Co L-edge spectrum for 100 Å Co/50 Å Cu/50 Å Co, with its absorption spectrum in the inset. The absorption spectra were obtained by subtracting the preedge region and scaling to unit step height above the L_2 edge.[1] The spin (M_s) and orbital (M_l) magnetic moments were obtained from the XMCD spectra, using sum rules and the areas under the L_3 and L_2 peaks,[1] namely,

$$M_s = \frac{(\Delta AL_3 - 2\Delta AL_2)}{C},$$

$$M_l = \frac{(\Delta AL_3 + \Delta AL_2)}{B}, \tag{1}$$

where ΔAL_3 and ΔAL_2 are the areas under the L_3 and L_2 peaks, and C and B are constants evaluated using the XMCD spectrum from Fig. 2(b). Because the Cu L_3 and L_2 areas are nearly the same, the induced magnetic moments are mainly spin derived, with a very small orbital magnetic contribution. Table I summarizes the moments for the nanoparticles and the films.

Figure 3 shows that the average spin moments for the thin films decrease with the film thickness. This has been observed previously[1,5] and it was attributed to the fact that the moment exists mainly at the interface and falls to zero within a few layers. The moments can be fitted with a function that has an inverse dependence on film thickness, as shown in the figure. The spin moments induced in the Cu nanoparticles depend critically on particle size with the value dropping by a third as the average particle size increased from ~26 to ~30 Å. The nanoparticle moments, as a function of particle diameter, are indicated in Fig. 3. From the figure, it can be seen that the average particle moment is significantly higher than that in films of the same thickness. The spin moments for the two ~30 Å sized nanoparticles with different densities were nearly the same, eliminating effects of particle-particle interactions.

The moments in nanoparticles are significantly higher than those in thin films of equivalent thicknesses. To understand this, we compute the spin moment in the nanoparticles by comparing the particle surface area to that of a thin film. This gives the average M_s in the nanoparticles as

$$M_s = \tfrac{3}{2}A\left(\Sigma_i \frac{n_i}{r_i}\right) \Big/ \Sigma_i n_i, \tag{2}$$

where the factor of 3/2 arises from the ratio of the surface areas of a sphere compared to a flat film with two interfaces. The constant A obtained from the fit shown in Fig. 3 is $0.147 \pm 0.016 \mu_B$ Å. The moment is weighted by the number

TABLE I. Spin and orbital magnetic moments extracted from the XMCD spectra of nanoparticles and thin films. The average sizes, standard deviations, and densities of the nanoparticles are listed. The Co moments for the 50 Å film serve as reference. Errors in the spin moments were estimated to be less than 10% based on the fits to the L_3 and L_2 peaks.

Sample	Atom	M_s (μ_B)	M_l (μ_B)
25.6 Å/10.1 Å	Co	1.39	0.14
$(6\pm0.4)\times10^{11}$ cm^{-2}	Cu	0.021	0.0014
29.4 Å/11.8 Å	Co	1.5	0.14
$(2.5\pm0.1)\times10^{11}$ cm^{-2}	Cu	0.008	0.0008
29.6 Å/16.8 Å	Co	1.54	0.14
$(0.8\pm0.1)\times10^{11}$ cm^{-2}	Cu	0.007	0.0007
	Co	1.64	0.14
Cu 50 Å film	Cu	0.005	0.0003
Cu 25 Å film	Cu	0.011	0.0009
Cu 13 Å film	Cu	0.013	0.0007
Cu 5 Å film	Cu	0.028	0.0017

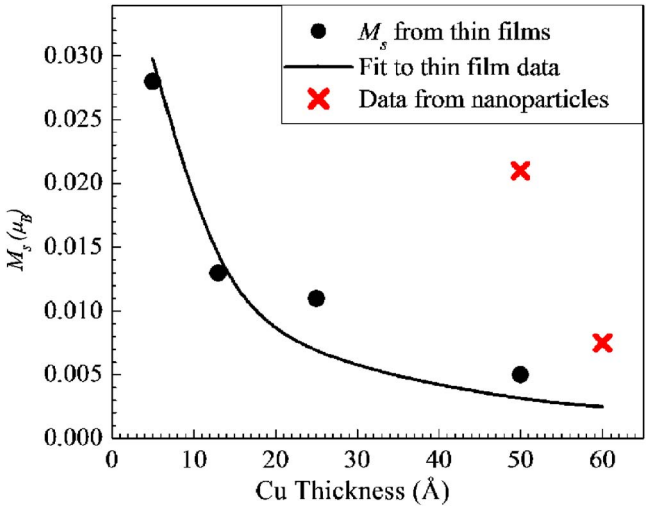

FIG. 3. (Color online) The spin moments for the thin films (●) as a function of film thickness t. The line is a fit using $1/t$ dependent function. The moments from the nanoparticles (×) are shown as a function of their diameter.

of particles n_i of radius r_i and summed over the distribution obtained from the TEM images. The calculated moments are $0.013\pm0.001\mu_B$ for the 25 Å particles and $0.009\pm0.001\mu_B$ for the 30 Å particles. The latter value is close to the observed values, the observed value for 25 Å particles is higher than the calculated one. This could be because we scale the moments for nanoparticles from thin films, ignoring changes in the nature of quantum confinement from one dimensional to three dimensional. Also, nonferromagnetic Au nanoparticles have been found to possess an intrinsic moment[17] that increases with decreasing particle size. For Au, this intrinsic moment was attributed to a Fermi hole effect at the particle surface and was inversely related to the Fermi wave vector.[18] It is likely that some of the Cu nanoparticles also possess an intrinsic moment, enhanced by the proximity of Co, leading to a higher average moment. The average spin moment in Co is lower in the nanoparticle samples compared to the thin films. This could reflect suppression by the Cu nanoparticles. This is higher for 25 Å particles because of the larger moment and higher surface coverage. As the particle size increases and coverage drops, the Co moment tends toward the bulk value.

The induced magnetization in Cu nanoparticles embedded in a Co matrix has been deduced using XMCD. The nanoparticles have spin moments more than double that of thin films of comparable thickness, related to the higher interfacial contact with the Co. The small particles may also possess an inherent magnetic moment enhanced by the ferromagnetic matrix. Studies of changes in magnetic behavior by changing the degree of quantum confinement in nanoparticles help in understanding the size effects on magnetism. By forming these structures on various magnetic substrates, it should be possible to understand effects of substrates as well and BLAG lends itself well to synthesize such systems. Combined with the elemental specificity of XMCD, it should deepen our understanding on magnetic interactions across an interface.

We thank Axel Hoffman and John Freeland for the discussions. The TEM imaging was carried out in the Center for Microanalysis of Materials of the Frederick Seitz Materials Research Laboratory, which is partially supported by the U.S. Department of Energy under Grant No. DEFG02-91-ER45439. The use of the Advanced Photon Source was supported by the U.S. Department of Energy, Office of Science, Office of Basic Energy Sciences under Contract No. DE-AC02-06CH11357.

[1] M. G. Samant, J. Stohr, S. S. P. Parkin, G. A. Held, B. D. Hermsmeier, F. Herman, M. van Schilfgaarde, L. C. Duda, D. C. Mancini, N. Wassdahl, and R. Nakajima, Phys. Rev. Lett. **72**, 1112 (1994).
[2] S. Pizzini, A. Fontaine, C. Giorgetti, E. Dartyge, J. F. Bobo, M. Piecuch, and F. Baudelet, Phys. Rev. Lett. **74**, 1470 (1995).
[3] T. Ohkochi, N. Hosoito, K. Mibu, and H. Hashizume, J. Phys. Soc. Jpn. **73**, 2212 (2004).
[4] J. W. Freeland, R. H. Kodama, M. Vedpathak, S. C. Erwin, D. J. Keavney, R. Winarski, P. Ryan, and R. A. Rosenberg, Phys. Rev. B **70**, 033201 (2004).
[5] G. A. Held, M. G. Samant, J. Stohr, S. S. P. Parkin, B. D. Hermsmeier, M. van Schilfgaarde, and R. Nakajima, Z. Phys. B: Condens. Matter **100**, 335 (1996).
[6] W. Weber, C. H. Back, A. Bischof, D. Pescia, and R. Allenspach, Nature (London) **374**, 788 (1995).
[7] S. S. P. Parkin, R. Bhadra, and K. P. Roche, Phys. Rev. Lett. **66**, 2152 (1991).
[8] G. A. Prinz, Science **282**, 1660 (1998).
[9] J. Stohr, J. Magn. Magn. Mater. **200**, 470 (1999).
[10] B. T. Thole, P. Carra, F. Sette, and G. van der Laan, Phys. Rev. Lett. **68**, 1943 (1992).
[11] P. Carra, B. T. Thole, M. Altarelli, and X. Wang, Phys. Rev. Lett. **70**, 694 (1993).
[12] H. Ebert, J. Stohr, S. S. P. Parkin, M. Samant, and A. Nilsson, Phys. Rev. B **53**, 16067 (1996).
[13] J. H. Weaver and G. D. Waddill, Science **251**, 1444 (1991).
[14] V. N. Antonov, J. S. Palmer, A. S. Bhatti, and J. H. Weaver, Phys. Rev. B **68**, 205418 (2003).
[15] A. S. Bhatti, V. N. Antonov, P. Swaminathan, J. S. Palmer, and J. H. Weaver, Appl. Phys. Lett. **90**, 011903 (2007).
[16] P. Swaminathan, V. N. Antonov, J. A. N. T. Soares, J. S. Palmer, and J. H. Weaver, Phys. Rev. B **73**, 125430 (2006).
[17] Y. Yamamoto, T. Miura, M. Suzuki, N. Kawamura, H. Miyagawa, T. Nakamura, K. Kobayashi, T. Teranishi, and H. Hori, Phys. Rev. Lett. **93**, 116801 (2004).
[18] H. Hori, Y. Yamamoto, T. Iwamoto, T. Miura, T. Teranishi, and M. Miyake, Phys. Rev. B **69**, 174411 (2004).